ISSN 1674-1056
http://cpb.iphy.ac.cn
http://iopscience.iop.org/cpb
中国物理 B
Chinese Physics
中国物理
Chinese Physics B

Controlling the entanglement of mechanical oscillators in composite optomechanical system

Jun Zhang(张俊), Qingxia Mu(穆青霞), Wen-Zhao Zhang(张闻钊)
Citation: Chin. Phys. B . 2018, 27(4): 040304. **doi:** 10.1088/1674-1056/27/4/040304

Journal homepage: http://cpb.iphy.ac.cn; http://iopscience.iop.org/cpb

What follows is a list of articles you may be interested in

Dynamics of entanglement protection of two qubits using a driven laser field and detunings: Independent and common, Markovian and/or non-Markovian regimes

S Golkar, M K Tavassoly
Chin. Phys. B . 2018, 27(4): 020303. **doi:** 10.1088/1674-1056/27/4/020303

Detecting high-dimensional multipartite entanglement via some classes of measurements

Lu Liu(刘璐), Ting Gao(高亭), Fengli Yan(闫凤利)
Chin. Phys. B . 2018, 27(2): 020306. **doi:** 10.1088/1674-1056/27/2/020306

Monogamy relations of quantum entanglement for partially coherently superposed states

Xian Shi(石现)
Chin. Phys. B . 2017, 26(12): 120303. **doi:** 10.1088/1674-1056/26/12/120303

Improving continuous-variable quantum key distribution under local oscillator intensity attack using entanglement in the middle

Fang-Li Yang(杨芳丽), Ying Guo(郭迎), Jin-Jing Shi(石金晶), Huan-Li Wang(王焕礼), Jin-Jin Pan(潘矜矜)
Chin. Phys. B . 2017, 26(10): 100303. **doi:** 10.1088/1674-1056/26/10/100303

Conditions on converting coherence into entanglement

Lian-Wu Yang(杨连武), Yun-Jie Xia(夏云杰)
Chin. Phys. B . 2017, 26(8): 080302. **doi:** 10.1088/1674-1056/26/8/080302

Controlling the entanglement of mechanical oscillators in composite optomechanical system*

Jun Zhang(张俊)[1], Qing-Xia Mu(穆青霞)[2], and Wen-Zhao Zhang(张闻钊)[3,†]

[1] School of Mathematics and Statistics, Guizhou University of Finance and Economics, Guiyang 550025, China
[2] Mathematics and Physics Department, North China Electric Power University, Beijing 102206, China
[3] Beijing Computational Science Research Center (CSRC), Beijing 100193, China

(Received 28 November 2017; revised manuscript received 18 January 2018; published online 10 March 2018)

A controllable entanglement scheme of two mechanical oscillators is proposed in a composite optomechanical system. In the case of strong driving and high dissipation, the dynamics of the movable mirror of the optomechanical cavity is characterized by an effective frequency in the long-time evolution of the system. Considering the classical nonlinear effects in an optomechanical system, we investigate the relationship between the effective frequency of the movable mirror and the adjustable parameters of the cavity. It shows that the effective frequency of the movable mirror can be adjusted ranging from ω_m (the resonance frequency of the coupling oscillator) to $-\omega_m$. Under the condition of experimental realization, we can generate and control steady-state entanglement between two oscillators by adjusting the effective frequency of the movable mirror and reducing the effective dissipation by selecting the parameter of the cavity driving laser appropriately. Our scheme provides a promising platform to control the steady-state behavior of solid-state qubits using classical manipulation, which is significant for quantum information processing and fundamental research.

Keywords: entanglement, optomechanics

PACS: 03.67.Mn, 42.50.–p, 03.67.Bg **DOI:** 10.1088/1674-1056/27/4/040304

1. Introduction

Quantum entanglement generation and control has been studied in various physical systems[1] such as electronic,[2,3] photonic,[4,5] and atomic and molecular systems,[6,7] ranging from microscopic systems to mesoscopic devices.[8] It can help us understand the fundamentals of quantum phenomena, such as quantum decoherence[9,10] and quantum-classical boundary.[11] In addition, it has wide applications in quantum information and quantum computation.[12,13]

Recently, there has been a great deal of interest in optomechanical systems which provides us with a convenient platform to realize macroscopic quantum effects.[14] Optomechanics explores the coupling between photons and phonons via radiation pressure. Because of the special coupling structure, optomechanics act as a coupling medium for diverse systems.[15–18] The interaction between photons and phonons can be used in mass sensors,[19] force and displacement detectors,[20] and the hardware for realizing quantum information processing.[12] Long distance photon entanglement can be used to construct quantum communication channels for secure information transmission.[21] The entanglement between the photons and solid bits,[22] such as mechanical oscillators and intracavitary atoms can realize the information interaction between flying bits and local bits,[23,24] as well as quantum information storage.[13]

Generating and controlling the entanglement of mechanical oscillators are also important subjects in the study of macroscopic quantum effects.[25,26] It is difficult for us to directly realize the parametric down-conversion (PDC) interaction between two mechanical oscillators in a system containing the interaction Hamiltonian of $V(b_1^\dagger + b_1)(b_2^\dagger + b_2)$. To achieve the effective mechanical interaction, the frequency difference between the mechanical oscillators should not be too large. Under this condition, the PDC interaction is very weak in comparison to the beam-splitter (BS) interaction in the dynamic system. In this case, it is hard to generate steady-state entanglement between oscillators. More recently, in order to prepare strongly entangled mechanical modes in the steady state, one can engineer the dissipation of the mechanical modes such that its steady state is the desired target state,[27–29] and we can also construct bilinear coupling in modulated optomechanics to create steady-state entanglement.[30] Usually, these schemes need to introduce extra quantum control, which increases the difficulty of the practical implementation of the entanglement proposals.

In this paper, we propose a convenient steady-state entanglement generating and controlling scheme for mechanical oscillators in a composite optomechanical system, in which the movable mirror of the optoemchanical cavity is coupled to a mechanical oscillator. By controlling the adjustable pa-

*Project supported by the National Natural Science Foundation of China (Grant Nos. 11704026 and 11461016), the Fund from Guizhou University of Finance and Economics, China (Grant No. 2017XZD01), and the Guizhou Youth Science and Technology Talent Development Project (Grant Nos. [2016] 170 and [2017] 150).

†Corresponding author. E-mail: zhangwz@csrc.ac.cn

© 2018 Chinese Physical Society and IOP Publishing Ltd

rameters of the classical driving laser, we are able to control the steady-state entanglement between two oscillators. In our analyses, the nonlinear optomechanical interaction, caused by radiation pressure, results in an effective frequency of the movable mirror in the optomechanical system. By choosing appropriate parameters, the effective frequency of the movable mirror can be reversed to $-\omega_m$. In this case, even though the frequency of two oscillators are the same, we can still enhance the PDC interaction and suppress the BS interaction, which generates steady-state entanglement.

2. Model and Hamiltonian

Considering an optomechanical system in which the movable mirror is coupled with a mechanical oscillator, as shown in Fig. 1, the Hamiltonian reads ($\hbar = 1$)

$$\begin{aligned} H &= H_{\rm sys} + H_{\rm d}, && (1)\\ H_{\rm sys} &= \omega_{\rm c} a^\dagger a + \sum_{j=1,2} \omega_{mj} b_j^\dagger b_j - g a^\dagger a (b_1^\dagger + b_1) \\ &\quad + V(b_1^\dagger + b_1)(b_2^\dagger + b_2), && (2)\\ H_{\rm d} &= \varepsilon(a^\dagger {\rm e}^{-{\rm i}\omega_{\rm d} t} + a {\rm e}^{{\rm i}\omega_{\rm d} t}), && (3) \end{aligned}$$

where a, b_1, and b_2 are the bosonic operators for the optical cavity, movable mirror, and coupled mechanical oscillator with frequencies $\omega_{\rm c}$, ω_{m1}, and ω_{m2} respectively. The single-photon coupling coefficient of the optomechanical interaction is $g = (\omega_c/L)\sqrt{\hbar/(2m\omega_m)}$. $H_{\rm d}$ describes the standard continuous-wave driving, $\omega_{\rm d}$ is the angular frequency of the laser and ε is the cavity driving strength, given by $\varepsilon \equiv 2\sqrt{P\kappa_{\rm ex}/(\hbar\omega_{\rm d})}$, with P being the input power of the laser and $\kappa_{\rm ex}$ being the input rate of the cavity. In the rotating frame under input laser frequency $\omega_{\rm d}$, we obtain the quantum Langevin equations,

$$\begin{aligned} \dot{a} &= -({\rm i}\Delta + \kappa/2)a + {\rm i}g a(b_1 + b_1^\dagger) + \sqrt{\kappa}a_{\rm in} - {\rm i}\varepsilon,\\ \dot{b_1} &= -({\rm i}\omega_{m1} + \gamma_1/2)b_1 + {\rm i}g a^\dagger a - {\rm i}V(b_2^\dagger + b_2) + \sqrt{\gamma_1}b_{{\rm in},1},\\ \dot{b_2} &= -({\rm i}\omega_{m2} + \gamma_2/2)b_2 - {\rm i}V(b_1^\dagger + b_1) + \sqrt{\gamma_2}b_{{\rm in},2}. \end{aligned} \quad (4)$$

For the purposes of discussion, we split the optical and mechanical field operators into the classical and quantum components: $a \to \alpha + \delta a$ and $b_1 \to \beta + \delta b_1$, where $\alpha \equiv \langle a \rangle$, $\beta \equiv \langle b_1 \rangle$. The time evolution of the annihilation operators of the system in the Heisenberg picture is then governed by

$$\begin{aligned} \dot{\alpha} &= -({\rm i}\Delta + \kappa/2)\alpha + {\rm i}g\alpha(\beta + \beta^*) - {\rm i}\varepsilon,\\ \dot{\beta} &= -({\rm i}\omega_{m1} + \gamma_1/2)\beta + {\rm i}g|\alpha|^2, && (5)\\ \dot{\delta a} &= -({\rm i}\Delta' + \kappa/2)\delta a + {\rm i}g\alpha(\delta b_1 + \delta b_1^\dagger),\\ &\quad + {\rm i}g\delta a(\delta b_1 + \delta b_1^\dagger) + \sqrt{\kappa}a_{\rm in},\\ \delta\dot{b}_1 &= -({\rm i}\omega_{m1} + \gamma_1/2)\delta b_1 + {\rm i}g(\alpha^*\delta a + \alpha\delta a^\dagger),\\ &\quad + {\rm i}g\delta a^\dagger\delta a - {\rm i}V(b_2^\dagger + b_2) + \sqrt{\gamma_1}b_{{\rm in},1},\\ \dot{b_2} &= -({\rm i}\omega_{m2} + \gamma_2/2)b_2 - {\rm i}V(\delta b_1^\dagger + \delta b_1)\\ &\quad + \sqrt{\gamma}b_{{\rm in},2} - 2{\rm i}V{\rm Re}(\beta), && (6) \end{aligned}$$

where $\Delta = \omega_{\rm c} - \omega_{\rm d}$ is the detuning between the driving field and the cavity frequency, $\Delta' = \Delta - g(\beta + \beta^*)$ is the effective detuning of the system. The nonlinear equations (5) dominate the coherent mean-field amplitude evolution of the system which depends on adjustable parameters Δ, κ, and ε. These parameters can be controlled by the input driving laser. Therefore, it is possible to control the quantum behavior of the system by utilizing the classical laser field. In blue sideband detuning $\Delta = \omega_{m1}$, the optomechanical system can be used to cool the mechanical oscillator.[31] In red sideband detuning $\Delta = -\omega_{m1}$, the optomechanical system can be used to generate entanglement between photons and phonons.[1] In strong driving condition $\varepsilon \gg \omega_{m1}$, the optical mode of the system can exhibit bistable and chaos behavior.[32] The nonlinear equations (6) dominate the quantum evolution of the system. The terms ${\rm i}g\alpha(\delta b_1 + \delta b_1^\dagger)$ and ${\rm i}g(\alpha^*\delta a + \alpha\delta a^\dagger)$ denote the field-enhanced linear interaction between optical mode and mechanical mode b_1. The linearized coupling rate $G = \alpha g$ depends on the dynamics of the classical part. The terms ${\rm i}g\delta a(\delta b_1 + \delta b_1^\dagger)$ and ${\rm i}g\delta a^\dagger\delta a$ denote the nonlinear interaction between the optical mode and the mechanical mode b_1. In addition, the average displacement of the mechanical oscillator, caused by the radiation pressure, $\langle x \rangle = \beta + \beta^* = 2{\rm Re}(\beta)$, will lead to a small shift of the detuning frequency $\Delta' = \Delta - g(\beta + \beta^*)$. It also adds a term of $2{\rm i}V{\rm Re}(\beta)$ as an equivalent driving on the coupled mechanical oscillator.

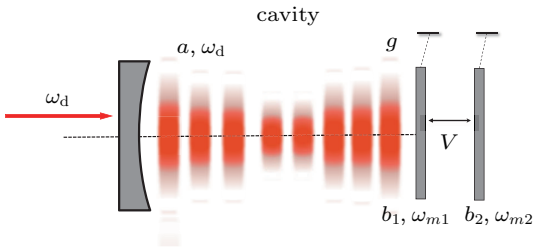


Fig. 1. (color online) Schematic diagram for the composite optomechanical system, where the optomenchnical oscillator is coupled to an additional mechanical oscillator. This three-mode bosonic system is used to prepare steady-state entanglement between modes b_1 and b_2. The cavity mode a is driven by a laser with frequency $\omega_{\rm d}$ and amplitude ε.

Currently, most experimental realizations of cavity optomechanics are still limited in the single-photon weak coupling with a strong driving condition.[33–35] Under this condition, for the quantum part, we can introduce the so-called "linearized" approximate description[14] of optomechanics when the nonlinear terms ${\rm i}g\delta a(\delta b_1 + \delta b_1^\dagger)$ and ${\rm i}g\delta a^\dagger\delta a$ can be omitted since they are relatively small with respect to the factor α. Thus, equation (6) can be formally integrated as

$$\begin{aligned} \delta a(t) &= \delta a(0){\rm e}^{-({\rm i}\Delta' + \kappa/2)}\\ &\quad + \int_0^t {\rm d}\tau {\rm e}^{-({\rm i}\Delta' + \kappa/2)(t-\tau)}[{\rm i}G(\delta b_1 + \delta b_1^\dagger) + \sqrt{\kappa}a_{\rm in}], \end{aligned}$$

$$\begin{aligned}\delta b_1(t) &= \delta b_1(0)\mathrm{e}^{-(\mathrm{i}\omega_{m1}+\gamma_1/2)t}+\int_0^t \mathrm{d}\tau \mathrm{e}^{-(\mathrm{i}\omega_{m1}+\gamma_1/2)(t-\tau)},\\ &\times[\mathrm{i}(G\delta a^\dagger+G^*\delta a)-V(b_2^\dagger+b_2)+\sqrt{\gamma_1}b_{\mathrm{in},1}]\\ b_2(t) &= b_2(0)\mathrm{e}^{-(\mathrm{i}\omega_{m2}+\gamma_2/2)t}+\int_0^t \mathrm{d}\tau \mathrm{e}^{-(\mathrm{i}\omega_{m2}+\gamma_2/2)(t-\tau)}\\ &\times[-V(\delta b_1^\dagger+\delta b_1)+\sqrt{\gamma_2}b_{\mathrm{in},2}-2\mathrm{i}V\mathrm{Re}(\beta)]. \end{aligned} \tag{7}$$

We consider the case of $\omega_{m1}\gg\{G,V\}$, i.e., the mode δb_1 is rapidly oscillating in evolution. Then the time evolution of $\delta b_1(t)$ can be approximately described as $\delta b_1(t)\approx\delta b_1(0)\mathrm{e}^{-(\mathrm{i}\omega_{m1}+\gamma_1/2)t}+B_{\mathrm{in},1}(t)$, where $B_{\mathrm{in},1}(t)=\int_0^t \mathrm{d}\tau \mathrm{e}^{-(\mathrm{i}\omega_{m1}+\gamma_1/2)(t-\tau)}\sqrt{\gamma_1}b_{\mathrm{in},1}(\tau)$. Substituting it into the equation of $\delta a(t)$, we have

$$\begin{aligned}\delta a(t) &= \delta a(0)\mathrm{e}^{-(\mathrm{i}\Delta'+\kappa/2)}+\int_0^t \mathrm{d}\tau \mathrm{e}^{-(\mathrm{i}\Delta'+\kappa/2)(t-\tau)}\\ &\times\mathrm{i}G[\delta b_1(0)\mathrm{e}^{-(\mathrm{i}\omega_{m1}+\gamma_1/2)\tau}+\mathrm{h.c.}]+A_{\mathrm{in}}. \end{aligned} \tag{8}$$

where $A_{\mathrm{in}}=\int_0^t \mathrm{d}\tau \mathrm{e}^{-(\mathrm{i}\Delta'+\kappa/2)(t-\tau)}[\mathrm{i}G(B_{\mathrm{in},1}+B_{\mathrm{in},1}^\dagger)+\sqrt{\kappa}a_{\mathrm{in}}]$ denotes the effective dissipation. Under the condition of $\kappa\gg\gamma_1$, the term containing $\mathrm{e}^{-\kappa t}$ is a fast decaying term, thus it can be neglected. Then we have

$$\begin{aligned}\delta a(t) &\approx \frac{\mathrm{i}G\delta b_1(t)}{\mathrm{i}(\Delta'-\omega_{m1})+(\kappa-\gamma_1)/2}\\ &+\frac{\mathrm{i}G\delta b_1^\dagger(t)}{\mathrm{i}(\Delta'+\omega_{m1})+(\kappa+\gamma_1)/2}+A_{\mathrm{in}}. \end{aligned} \tag{9}$$

We consider the case of $\Delta'\approx\omega_{m1}$, where the second term can be ignored as a higher order small quantity.

$$\delta a(t)\approx\frac{\mathrm{i}G\delta b_1(t)}{\mathrm{i}(\Delta'-\omega_{m1})+(\kappa-\gamma_1)/2}+A_{\mathrm{in}}. \tag{10}$$

Substituting $\delta a(t)$ into Eqs. (6), we find that the dynamics of modes b_1 and b_2 are independent of mode a. From Eqs. (6) we obtain the approximated expressions,

$$\begin{aligned}\delta\dot{b}_1 &= -(\mathrm{i}\omega_{\mathrm{eff}}+\gamma_{\mathrm{eff}}/2)\delta b_1-\mathrm{i}V(b_2^\dagger+b_2)+\sqrt{\gamma_{\mathrm{eff}}}B'_{\mathrm{in},1},\\ \dot{b}_2 &= -(\mathrm{i}\omega_{m2}+\gamma_2/2)b_2-\mathrm{i}V(\delta b_1^\dagger+\delta b_1)\\ &+\sqrt{\gamma}b_{\mathrm{in},2}-2\mathrm{i}V\mathrm{Re}(\beta), \end{aligned} \tag{11}$$

where $\omega_{\mathrm{eff}}=\omega_{m1}-\xi(\Delta'-\omega_{m1})$ denotes the effective frequency of the movable mirror, $\gamma_{\mathrm{eff}}=\gamma_{m1}+\xi(\kappa-\gamma_1)$ denotes the effective dissipation of the movable mirror, $\xi=|G|^2/[(\Delta'-\omega_{m1})^2+(\kappa-\gamma_1)^2/4]$ is the effective amplification factor caused by the optomechanical interaction, $B'_{\mathrm{in},1}=\int_0^t d\tau \mathrm{e}^{-(\mathrm{i}\omega_{m1}+\gamma_1/2)(t-\tau)}[\mathrm{i}(G^*A_{\mathrm{in}}+GA_{\mathrm{in}}^\dagger)+\sqrt{\gamma_1}b_{\mathrm{in},1}]$ is the effective damping of the movable mirror. Thus, the effective Hamiltonian is

$$H_{\mathrm{eff}}=\omega_{\mathrm{eff}}\delta b_1^\dagger\delta b_1+\omega_{m2}b_2^\dagger b_2+V(\delta b_1^\dagger+\delta b_1)(b_2^\dagger+b_2). \tag{12}$$

In addition, the mean value β causes an effective driving on the coupled oscillator, i.e. $2\mathrm{i}V\,\mathrm{Re}(\beta)$. This equivalent driving is a coherent driving which can be used to enhance the mean number of the coupled oscillator. The effective frequency ω_{eff} is no longer a fixed parameter. Instead, it can be controlled by the laser driving strength ε and detuning Δ. Thus, it is possible to control the quantum behavior between the two oscillators.

3. Controlling the entanglement of mechanical oscillators

As one can tell, the effective frequency ω_{eff} is a function of G and frequency detuning Δ. Thus, the optical driving field can indirectly modulate the frequency of the movable mirror through the interaction from radiation pressure. When $\omega_{\mathrm{eff}}=\omega_{m2}$, analogous to the anti-Stokes regime, BS interaction is on resonance in the system, i.e., $V(b_1^\dagger b_2+\mathrm{h.c.})$. This interaction will cause the state transfer between the oscillators, sideband cooling, etc.[35,36] When $\omega_{\mathrm{eff}}=-\omega_{m2}$, analogous to the Stokes regime, PDC interaction is on resonance in the system, i.e. $V(b_1^\dagger b_2^\dagger+\mathrm{h.c.})$. This interaction will cause the entanglement of mechanical oscillators, squeeze of mechanical oscillators, etc.[1,37] Noting that since we select Δ' approximately equal to ω_{m1}, ξ should be large enough to make $\omega_{\mathrm{eff}}=-\omega_{m2}$, so that the effective dissipation γ_{eff} will also be magnified. In order to get a large value of ξ and reduce the effective dissipation, a larger G is needed, which means, a strong driving strength ε and a small dissipation rate κ are needed.

The interaction between light and mechanical motion due to radiation pressure is intrinsically nonlinear. Several theoretical studies of the nonlinear effect in optomechanical systems have been reported recently.[13,32,38] Although we have used the linearized approximation in the quantum part, for rigorous consideration, especially for strong driving condition, we should also examine the nonlinear behavior of the optomechanical system when discussing the quantum effect between the two oscillators. Without losing generality, we set $\omega_{m1}=\omega_{m2}=\omega_m$ in the following discussion. To study the nonlinear behavior of the system, we first consider the classical part of the dynamics, i.e., Eqs. (5). In the steady state they read,

$$\begin{aligned}0 &= -(\mathrm{i}\Delta+\kappa/2)\alpha+\mathrm{i}g\alpha(\beta+\beta^*)-\mathrm{i}\varepsilon,\\ 0 &= -(\mathrm{i}\omega_m+\gamma_1/2)\beta+\mathrm{i}g|\alpha|^2. \end{aligned} \tag{13}$$

Combining the above equations we obtain a third-order polynomial root equation for the mean-field cavity occupation,

$$0=4\chi^2n^3-4\Delta\chi n^2+(\Delta^2+\kappa^2/4)n-\varepsilon^2, \tag{14}$$

where $n=|\alpha|^2$ is the mean photon number in the cavity, and $\chi=g^2/(\omega_m+\gamma_1^2/4\omega_m)$ is the nonlinear parameter. This equation is commonly used to discuss the bistability of the optomechanical system.[13,32,38] Equation (14) indicates that the mean-field equations have either one or three solutions depending on the number of real roots of the polynomial. As

shown in Fig. 2, we exhibit the bistability behavior of the linearized coupling rate G as a function of driving strength ε, single-photon coupling rate g, detuning Δ, and cavity dissipation rate κ (the black dashed line denotes the metastable state solution,[32] the same as in Fig. 3). The same behavior has also been discussed in Ref. [32]. We can obtain a strong linearized coupling rate $G \approx 0.7\omega_m$, in weak single-photon coupling rate and large dissipation rate regime. When using ε and G to adjust the value of $\omega_{\rm eff}$, we need to ensure that the condition $G \ll \omega_{m1}$ is satisfied to ensure the rationality of the approximation. The solution corresponding to the blue-solid line in Figs. 2(a) and 2(b) meets our needs. Therefore, in the following discussion, we will only deal with the steady state solution corresponding to the blue-solid line and ignore others.

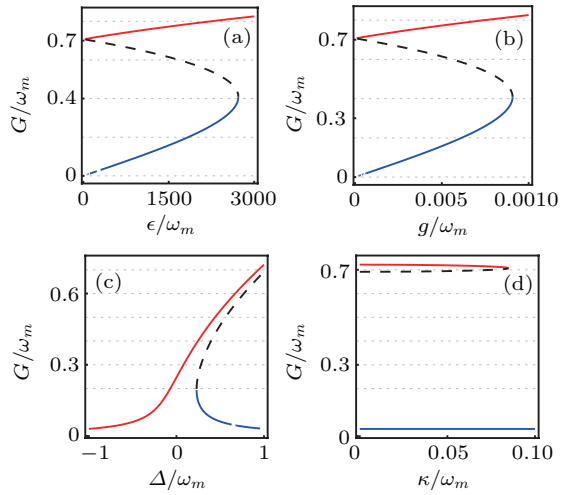


Fig. 2. (color online) (a) The coupling rate G as a function of driving strength ε, where $\Delta = \omega_m$, $g/\omega_m = 10^{-4}$, $\gamma_1/\omega_m = 10^{-5}$, and $\kappa/\omega_m = 10^{-2}$. (b) G as a function of single-photon coupling rate g, where $\Delta = \omega_m$, $\varepsilon/\omega_m = 10^3$, $\gamma_1/\omega_m = 10^{-5}$, and $\kappa/\omega_m = 10^{-2}$. (c) G as a function of detuning frequency Δ, where $g/\omega_m = 10^{-4}$, $\varepsilon/\omega_m = 10^3$, $\gamma_1/\omega_m = 10^{-5}$, and $\kappa/\omega_m = 10^{-2}$. (d) G as a function of dissipation rate κ, where $\Delta = \omega_m$, $g/\omega_m = 10^{-4}$, $\gamma_1/\omega_m = 10^{-5}$, and $\varepsilon/\omega_m = 10^3$.

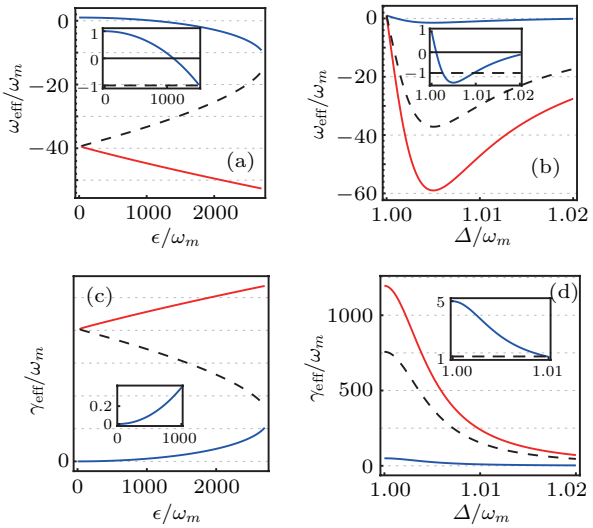


Fig. 3. (color online) (a) and (c) Effective frequency $\omega_{\rm eff}$ and effective dissipation rate $\gamma_{\rm eff}$ as a function of driving strength ε. The detuning frequency $\Delta/\omega_m = 1.01$. (b) and (d) $\omega_{\rm eff}$ and $\gamma_{\rm eff}$ as a function of detuning frequency Δ. The driving strength $\varepsilon/\omega_m = 1.5 \times 10^3$. Other parameters are $g/\omega_m = 10^{-4}$, $\kappa/\omega_m = 10^{-2}$, and $\gamma_1/\omega_m = 10^{-5}$.

The corresponding bistable behavior of the effective frequency $\omega_{\rm eff}$ and the effective dissipation rate $\gamma_{\rm eff}$ are shown in Fig. 3. In Figs. 3(a) and 3(b), we plot the effective frequency $\omega_{\rm eff}$ as a function of ε and Δ, showing an obvious bistable behavior of $\omega_{\rm eff}$. We can adjust the effective frequency from ω_{m2} to $-\omega_{m2}$ by increasing driving strength and frequency detuning. In Figs. 3(c) and 3(d), we plot the effective frequency $\gamma_{\rm eff}$ as a function of ε and Δ, showing an obvious bistable behavior of $\gamma_{\rm eff}$. The effective damping rate increases with the increase of the driving strength, and decreases with the increase of the detuning frequency.

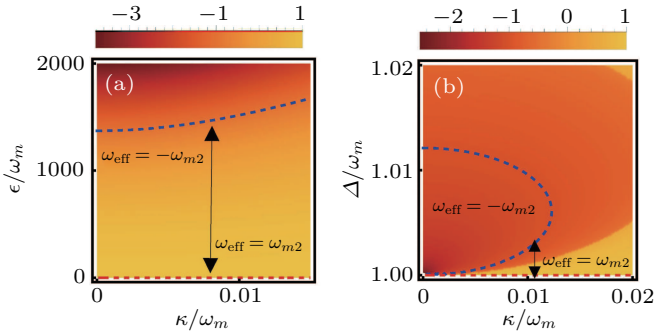


Fig. 4. (color online) Effective frequency $\omega_{\rm eff}$ as a function of ε, Δ, and κ. (a) $\omega_{\rm eff}$ as a function of ε and κ, the red-dashed line denotes $\omega_{\rm eff} = \omega_m$ and the blue-dashed line denotes $\omega_{\rm eff} = -\omega_m$. The detuning frequency $\Delta/\omega_m = 1.01$. (b) $\omega_{\rm eff}$ as a function of Δ and κ, the red-dashed line denotes $\omega_{\rm eff} = \omega_m$ and the blue-dashed line denotes $\omega_{\rm eff} = -\omega_m$. The driving strength $\varepsilon/\omega_m = 1.6 \times 10^3$. Other parameters are the same as those in Fig. 3.

Considering the effect of cavity dissipation rate κ, we plot the density graph of $\omega_{\rm eff}$ as a function of ε, κ, and Δ, κ in Figs. 4(a) and 4(b), respectively. The blue-dashed line indicates $\omega_{\rm eff} = -\omega_{m2}$, and the red-dashed line indicates $\omega_{\rm eff} = \omega_{m2}$. As shown in Fig. 4(a), with the increase of the driving strength, the effective frequency will shift from the intrinsic frequency of the oscillator to the negative frequency. It is worth noting that the value of driving strength $\varepsilon = 0$ cannot be achieved in our approximation. We draw from $\varepsilon = 0$ only for the completeness of the figure. As shown in the blue-dashed line, when the driving strength is large enough, the effective frequency becomes $-\omega_{m2}$, and the original BS interaction turns into PDC interaction. In addition, to achieve $\omega_{\rm eff} = -\omega_{m2}$, we need to increase the driving strength with the increase of dissipation rate. Shown as the red-dashed line in Fig. 4(b), when the detuning frequency of the cavity is equal to the oscillator frequency ω_{m2}, the resonance amplification occurs. Under this condition, the amplification rate ε reaches maximum, but the effective frequency is not shifted, which can also be told from the expression of $\omega_{\rm eff}$. Shown as the blue-dashed line, the effective frequency can reach the value $-\omega_m$ under the proper detuning frequency Δ. However, when the dissipation is too large, the optomechanical interaction is not sufficient to make the effective frequency equal to $-\omega_m$. Thus, under the given driving strength, the effective frequency can reach $-\omega_m$ with the appropriate detuning frequency. Con-

sidering the results in comprehensively, by properly increasing the detuning frequency, the effective frequency $\omega_{\rm eff}$ can achieve $-\omega_m$ and the effective dissipation $\gamma_{\rm eff}$ can be reduced under the given driving strength. The above analysis shows that, it is possible to adjust the effective frequency from ω_{m2} to $-\omega_{m2}$ by controlling the driving strength ε and detuning Δ. Especially for the case $\omega_{\rm eff} = -\omega_m$, the system can be used to generate entanglement between two oscillators.

With the help of the effective Hamiltonian, we investigate the entanglement between the two oscillators. For a nonchaotic dynamical process, the properties of the quantum fluctuations can be determined from a 4×4 covariance matrix, $\dot{V}(t) = A(t)V(t) + V(t)A^{\rm T}(t) + D$, where the elements of the covariance matrix are defined as $V_{ij} = \langle u_i u_j + u_j u_i\rangle$, $u = (\delta x_1, \delta p_1, x_2, p_2)^{\rm T}$, and $D = {\rm diag}(0, \gamma_{\rm eff}(2n_{\rm th1}+1), 0, \gamma_2(2n_{\rm th2}+1) + 4V{\rm Re}(\beta))$

$$A = \begin{pmatrix} 0 & \omega_{\rm eff} & 0 & 0 \\ -\omega_{\rm eff} & -\gamma_{\rm eff} & -V & 0 \\ 0 & 0 & 0 & \omega_{m2} \\ -V & 0 & -\omega_{m2} & -\gamma_2 \end{pmatrix}. \tag{15}$$

Thus, the degree of quantum entanglement between the mechanical and optical modes can be assessed by calculating the so-called logarithmic negativity,[39] defined as $E_n \equiv \max[0, -\ln(2\eta^-)]$, where $\eta^- \equiv (1/\sqrt{2})[\Sigma(V) - \sqrt{\Sigma(V)^2 - 4\det V}]^{1/2}$ and $\Sigma(V) = \det(V_A) + \det(V_B) - 2\det(V_C)$. The matrix V_A, V_B, and V_C are 2×2 matrices related to the covariance matrix V as

$$V = \begin{pmatrix} V_A & V_C \\ V_C^{\rm T} & V_B \end{pmatrix}. \tag{16}$$

We plot the logarithmic negativity E_n as a function of optical driving strength ε and frequency detuning Δ with different oscillator coupling strength V in Fig. 5. Note that the linearized optomechanical interaction can lead to a cooling process.[31] Combining with the phonon–phonon parametric coupling, the system can cool the mechanical modes b_1 and b_2 into an entangled state in the steady state. Therefore, we have the reason to choose the thermal phonon number of the movable mirror to be equal to zero. As shown in Fig. 5(a), for a particular coupling strength V, the peak of entanglement appears when the driving strength is around $1550\omega_m$. Under this driving strength, the effective frequency $\omega_{\rm eff} = -\omega_m$ (this result can be obtained from Fig. 4(a)) which is consistent with the conclusions we have discussed above. It means that we can achieve the purpose of controlling the entanglement of the oscillators by adjusting the driving strength of the cavity. In addition, the degree of the entanglement increases with the oscillator coupling strength V. As shown in Fig. 5(b), for a particular coupling strength V, the peak of entanglement appears at the frequency detuning around $1.012\omega_m$. Under this frequency detuning, the effective frequency $\omega_{\rm eff} = -\omega_m$ (this result can be obtained from Fig. 4(b)) which is consistent with the conclusions we have discussed above. This means that we can achieve the purpose of controlling the entanglement of the oscillators by adjusting the frequency detuning of the optical cavity. Again the entanglement increases with the oscillator coupling strength V.

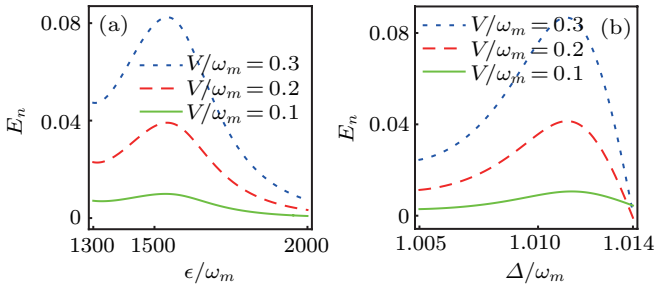


Fig. 5. (color online) (a) Entanglement E_n as a function of ε with different coupling V. The detuning frequency $\Delta/\omega_m = 1.01$. (b) E_n as a function of ε with different coupling V. The driving strength $\varepsilon/\omega_m = 1.6\times 10^3$. Other parameters are $g/\omega_m = 10^{-4}$, $\kappa/\omega_m = 10^{-2}$, $\gamma_1/\omega_m = \gamma_2/\omega_m = 10^{-5}$, $n_{\rm th1} = n_{\rm th2} = 0$.

4. Discussion and conclusion

In the present experimental conditions, the mass and scale of the mechanical oscillator can achieve macroscopic level in suspended mirror optomechanical system.[8,14] The coupling between mechanical resonators can be realized in geometrically interconnected beams[40] and a charged mechanical resonator via Coulomb interaction.[41] Therefore, our system has potential applications for the generation and controling of macroscopic entanglement. Under the current experimental conditions, the coherent phonon manipulation in coupled mechanical resonators is difficult to realize. One can utilize two GaAs-based mechanical resonators by using a piezoelectric transducer[40] or two superconducting lumped-element electrical resonators using an RF SQUID-mediated tunable coupler.[42] In our scheme, a more convenient way to manipulate the mechanical resonators has been proposed, with which one only needs to control the adjustable parameters of the classical driving laser.

In our result, we proposed a scheme to generate and control the entanglement between two oscillators in a composite optomechanical system. It shows that, under the condition $\kappa \gg \gamma_1$, the radiation pressure from the optical mode can cause an effective frequency $\omega_{\rm eff}$ of the mechanical mirror. The mean value of the movable mirror acts as an effective driving on the coupled oscillator. In addition, this effective frequency can be controlled by the classical optical driving, i.e., driving strength ε and frequency detuning Δ. In the case of anti-Stokes regime $\Delta' \approx \omega_{m1}$, the effective frequency of the movable mirror can be adjusted from ω_m to $-\omega_m$ and the phonon can be cooled to the ground state. Then, we can generate the steady state entanglement between two oscillators by setting the effective frequency $\omega_{\rm eff} = -\omega_{m2}$, which corresponds to the parametric down-conversion process. Manipulating the effective frequency $\omega_{\rm eff}$ and coupling strength V we can control the

strength of the entanglement. Our scheme provides a more convenient way to generate and control the steady state entanglement of mechanical oscillators, which has potential applications in quantum control and fundamental research.

Acknowledgments

We would like to thank Prof. Jing An and Dr. Lei-Ming Zhou for our helpful discussions.

References

[1] Cheng J, Zhang W Z, Zhou L and Zhang W 2016 *Sci. Rep.* **6** 23678
[2] Cerletti V, Gywat O and Loss D 2005 *Phys. Rev. B* **72** 115316
[3] Wang C, Zhang Y and Jin G S 2011 *Phys. Rev. A* **84** 032307
[4] Sangouard N, Simon C, Coudreau T and Gisin N 2008 *Phys. Rev. A* **78** 050301
[5] Wang G, Huang L, Lai Y C and Grebogi C 2014 *Phys. Rev. Lett.* **112** 110406
[6] Slodička L, Hétet G, Röck N, Schindler P, Hennrich M and Blatt R 2013 *Phys. Rev. Lett.* **110** 083603
[7] Nicacio F, Furuya K and Semião F L 2013 *Phys. Rev. A* **88** 022330
[8] Liao J Q and Tian L 2016 *Phys. Rev. Lett.* **116** 163602
[9] Beau M, Kiukas J, Egusquiza I L and del Campo A 2017 *Phys. Rev. Lett.* **119** 130401
[10] Pikovski I, Zych M, Costa F and Brukner Č 2015 *Nat. Phys.* **11** 668
[11] Zurek W H 2003 *Rev. Mod. Phys.* **75** 715
[12] Chen T Y, Zhang W Z, Fang R Z, Hang C Z and Zhou L 2017 *Opt. Express* **25** 10779
[13] Zhang W Z, Cheng J, Liu J Y and Zhou L 2015 *Phys. Rev. A* **91** 063836
[14] Aspelmeyer M, Kippenberg T J and Marquardt F 2014 *Rev. Mod. Phys.* **86** 1391
[15] Chen X, Liu Y C, Peng P, Zhi Y and Xiao Y F 2015 *Phys. Rev. A* **92** 033841
[16] Fong K Y, Fan L, Jiang L, Han X and Tang H X 2014 *Phys. Rev. A* **90** 051801
[17] Dong Y, Ye J and Pu H 2011 *Phys. Rev. A* **83** 031608
[18] Heikkilä T T, Massel F, Tuorila J, Khan R and Sillanpää M A 2014 *Phys. Rev. Lett.* **112** 203603
[19] He Y 2015 *Appl. Phys. Lett.* **106** 121905
[20] Zhang W Z, Han Y, Xiong B and Zhou L 2017 *New J. Phys.* **19** 083022
[21] Černotík O C V and Hammerer K 2016 *Phys. Rev. A* **94** 012340
[22] Liao J Q, Wu Q Q and Nori F 2014 *Phys. Rev. A* **89** 014302
[23] Lian J, Liu N, Liang J Q, Chen G and Jia S 2013 *Phys. Rev. A* **88** 043820
[24] Stannigel K, Rabl P, Sørensen A S, Lukin M D and Zoller P 2011 *Phys. Rev. A* **84** 042341
[25] Thompson J D, Zwickl B M, Jayich A M, Marquardt F, Girvin S M and Harris J G E 2008 *Nature* **452** 72
[26] Mu Q, Zhao X and Yu T 2016 *Phys. Rev. A* **94** 012334
[27] Wang Y D and Clerk A A 2013 *Phys. Rev. Lett.* **110** 253601
[28] Tan H, Li G and Meystre P 2013 *Phys. Rev. A* **87** 033829
[29] Woolley M J and Clerk A A 2014 *Phys. Rev. A* **89** 063805
[30] Wang M, Lü X Y, Wang Y D, You J Q and Wu Y 2016 *Phys. Rev. A* **94** 053807
[31] Liu Y C, Liu R S, Dong C H, Li Y, Gong Q and Xiao Y F 2015 *Phys. Rev. A* **91** 013824
[32] Ghobadi R, Bahrampour A R and Simon C 2011 *Phys. Rev. A* **84** 033846
[33] Gröblacher S, Hammerer K, Vanner M R and Aspelmeyer M 2009 *Nature* **460** 724
[34] Chan J, Alegre T P M, Safavi-Naeini A H, Hill J T, Krause A, Gröblacher S, Aspelmeyer M and Painter O 2011 *Nature* **478** 89
[35] Teufel J D, Donner T, Li D, Harlow J W, Allman M S, Cicak K, Sirois a J, Whittaker J D, Lehnert K W and Simmonds R W 2011 *Nature* **475** 359
[36] U S S and Narayanan A 2013 *Phys. Rev. A* **88** 033802
[37] Qu K and Agarwal G S 2015 *Phys. Rev. A* **91** 063815
[38] Doolin C, Hauer B D, Kim P H, MacDonald A J R, Ramp H and Davis J P 2014 *Phys. Rev. A* **89** 053838
[39] Plenio M B 2005 *Phys. Rev. Lett.* **95** 090503
[40] Okamoto H, Gourgout A, Chang C Y, Onomitsu K, Mahboob I, Chang E Y and Yamaguchi H 2013 *Nat. Phys.* **9** 598
[41] Ma P C, Zhang J Q, Xiao Y, Feng M and Zhang Z M 2014 *Phys. Rev. A* **90** 043825
[42] Tian L, Allman M S and Simmonds R W 2008 *New J. Phys.* **10** 115001